J|A|C|S
ARTICLES
Published on Web 01/28/2006

Structural Evolution in a Hydrothermal Reaction between Nb_2O_5 and NaOH Solution: From Nb_2O_5 Grains to Microporous $Na_2Nb_2O_6 \cdot {}^2/_3H_2O$ Fibers and $NaNbO_3$ Cubes

Huaiyong Zhu,*,† Zhanfeng Zheng,† Xueping Gao,*,‡ Yining Huang,§ Zhimin Yan,§ Jin Zou,|| Hongming Yin,⊥ Qingdi Zou,⊥ Scott H. Kable,⊥ Jincai Zhao,# Yunfei Xi,† Wayde N. Martens,† and Ray L. Frost†

Contribution from the Inorganic Materials Research Program, School of Physical and Chemical Sciences, Queensland University of Technology, GPO Box 2434, Brisbane, QLD 4001, Australia, Institute of New Energy Material Chemistry, Department of Materials Chemistry, Nankai University, Tianjin 300071, China, Department of Chemistry, University of Western Ontario, London, Ontario, Canada N6A 5B7, School of Engineering and Centre for Microanalysis and Microscopy, The University of Queensland, St Lucia, QLD 4072 Australia, School of Chemistry, The University of Sydney, NSW 2006, Australia, and Institute of Chemistry, The Chinese Academy of Science, Beijing 100080, China

Received September 19, 2005; E-mail: hy.zhu@qut.edu.au; xpgao@nankai.edu.cn

Abstract: Niobium pentoxide reacts actively with concentrate NaOH solution under hydrothermal conditions at as low as 120 °C. The reaction ruptures the corner-sharing of NbO_7 decahedra and NbO_6 octahedra in the reactant Nb_2O_5, yielding various niobates, and the structure and composition of the niobates depend on the reaction temperature and time. The morphological evolution of the solid products in the reaction at 180 °C is monitored via SEM: the fine Nb_2O_5 powder aggregates first to irregular bars, and then niobate fibers with an aspect ratio of hundreds form. The fibers are microporous molecular sieve with a monoclinic lattice, $Na_2Nb_2O_6 \cdot {}^2/_3H_2O$. The fibers are a metastable intermediate of this reaction, and they completely convert to the final product $NaNbO_3$ cubes in the prolonged reaction of 1 h. This study demonstrates that by carefully optimizing the reaction condition, we can selectively fabricate niobate structures of high purity, including the delicate microporous fibers, through a direct reaction between concentrated NaOH solution and Nb_2O_5. This synthesis route is simple and suitable for the large-scale production of the fibers. The reaction first yields poorly crystallized niobates consisting of edge-sharing NbO_6 octahedra, and then the microporous fibers crystallize and grow by assembling NbO_6 octahedra or clusters of NbO_6 octahedra and NaO_6 units. Thus, the selection of the fibril or cubic product is achieved by control of reaction kinetics. Finally, niobates with different structures exhibit remarkable differences in light absorption and photoluminescence properties. Therefore, this study is of importance for developing new functional materials by the wet-chemistry process.

I. Introduction

Alkaline niobates have emerged as a novel material with enormous technological and scientific interest because of their excellent nonlinear optical, ferroelectric, piezoelectric, electric-optic, ionic conductivity, pyroelectric, photorefractive, selective ion exchange, and photocatalytic properties.[1−5] For instance, potassium/sodium niobates are potential substitutes for the lead zirconium titanate (PZT) as high-performance piezoelectric ceramics because of their piezoelectric characteristics and the feature that they are lead free.[1] Large lead content in the PZT materials causes serious concerns about environment pollution during the fabrication, use, and disposal of the materials. The alkaline niobates have many potential applications such as acoustic transducers, delay lines and filters, optical modulators, second harmonic generators, Q-switches, beam deflectors, phase conjugators, dielectric waveguides, holographic data storage, and selective ion exchanger for sequestration of hazardous divalent metals.[6−10] Meanwhile, the great potential of these

† Queensland University of Technology.
‡ Nankai University.
§ University of Western Ontario.
|| The University of Queensland.
⊥ The University of Sydney.
The Chinese Academy of Science.

(1) Saito, Y.; Takao, H.; Tani, T.; Nonoyama, T.; Takatori, K.; Homma, T.; Nagaya, T.; Nakamura, M. *Nature* **2004**, *432*, 84.
(2) Domen, K.; Kudo, A.; Shibata, M.; Tanaka, A.; Maruya, K.; Onishi, T. *J. Chem. Soc., Chem. Commun.* **1986**, 1706.
(3) Qiao, H.; Xu, J.; Zhang, G.; Zhang, X.; Sun, Q.; Zhang, G. *Phys. Rev. B: Condens. Matter* **2004**, *70*, 094101.
(4) Nyman, M.; Bonhomme, F.; Alam, T. M.; Rodriguez, M. A.; Cherry, B. R.; Krumhansl, J. L.; Nenoff, T. M.; Sattler A. M. *Science* **2002**, *297*, 996.
(5) An, C.; Tang, K.; Wang, C.; Shen, G.; Qian, Y. T. *Mater. Res. Bull.* **2002**, *37*, 1791.
(6) Feigelson, R. S. *J. Cryst. Growth* **1996**, *166*, 1.
(7) Maciel, G. S.; Rakov, N.; de Araujo, C. B.; Lipovskii, A. A.; Tagantsev, D. K. *Appl. Phys. Lett.* **2001**, *79*, 584.
(8) Cho, C.-R.; Katardjiev, I.; Grishin, M.; Grishin, A. *Appl. Phys. Lett.* **2002**, *80*, 3171.
(9) Blomqvist, M.; Khartsev, S.; Grishin, A.; Petraru, A.; Buchal, C. *Appl. Phys. Lett.* **2003**, *82*, 439.

materials has also stimulated research on their synthesis.[10−20] Alkaline niobate powders are usually synthesized by a solid-state reaction of heating alkaline carbonates and niobium pentoxide (Nb_2O_5) at temperatures of 800 °C or above[1−3,5−8] because Nb_2O_5 was generally regarded as a "refractory" mineral substance, which only reacts with concentrated hydrofluoric acid and fused alkali.[21,22] Sol−gel methods, using alkoxide precursors and complexes with organic compounds, hence were also reported for the alkaline niobate synthesis.[10,13−15] Kormarneni et al.[16] found that niobium oxide powder reacted with an aqueous solution of potassium hydroxide (KOH) at 194 °C to yield crystalline $KNbO_3$. An outstanding advantage of such a hydrothermal synthesis is that the reaction temperature required to produce niobate crystalline is much lower than those in other methods. Recently, potassium niobates $K_4Nb_6O_{17}$ and $KNbO_3$, and sodium niobate, $NaNbO_3$, were synthesized by the reaction of Nb_2O_5 solid with concentrate aqueous potassium hydroxide (KOH) or sodium hydroxide (NaOH) solution under hydrothermal conditions, yielding potassium niobates, $K_4Nb_6O_{17}$ and $KNbO_3$,[17,18] and sodium niobate, $NaNbO_3$, respectively.[19,20]

In recent years, it has been found that the reaction between fine metal oxide powder or precipitate of a transition metal hydrate and concentrated NaOH solution under moderate hydrothermal conditions is an effective approach to achieve one-dimensional (1D) structures of metal oxides and hydroxides with nanometer-scale dimensions.[23−27] There is significant interest in these 1D-nanostructures, such as fibers and tubes of transition metal oxides,[23−31] because the nanostructures, representing the transition from inorganic "molecules" (or crystal unit cells) to bulk solid materials, could exhibit novel reaction behaviors and physicochemical properties.[32−34] However, in the reported hydrothermal syntheses involving NaOH solution, the attention was focused on the final products when the reaction reached equilibrium,[4,10,13−27,29] while the structure evolution from the solid reactant to the intermediate and final product during the reaction remains unexplored. Consequently, the reaction kinetics has not been deliberately controlled to achieve delicate new structures. In the present study, we investigate the structural evolution during the reaction between Nb_2O_5 powder and concentrated aqueous NaOH solution under hydrothermal conditions. Such a structural evolution provides a marvelous opportunity for selecting the niobate products with the desired morphologies and structures through kinetic control of the reaction. In such a reaction at an optimized temperature, the fine Nb_2O_5 powder aggregates first to irregular bars, and as the reaction advances the aspect ratio (length to the thickness) of the bars increases slightly. Next, niobate fibers with an aspect ratio of hundreds form at the expense of the bars, and finally the fibers convert to cubes. The fibers are found to be microporous niobate molecular sieves with a formula of $Na_2Nb_2O_6{\cdot}^2/_3H_2O$, being distinctly different from the cubes of $NaNbO_3$, in terms of composition, shape, crystal phase, and ion exchange ability. The microporous molecular sieves $Na_2Nb_{1-x}Ti_xO_6(OH)_x{\cdot}H_2O$, consisting of octahedra of NaO_6, NbO_6, and TiO_6, were first synthesized by Nyman et al.[10,13] from niobium alkoxides of niobium and titanium, as a novel class of molecular sieves (so-called Sandia Octahedral Molecular Sieves, abbreviated as SOMS). They are selective ion exchangers for sequestration of nuclear waste, radioactive Sr^{2+} ions. However, SOMS with low concentration (<5%) of substitute M^{IV} ($M \simeq Ti, Zr$) are unstable and difficult to obtain in a pure sodium niobate form.[13] Recently, the end-member of the series, $Na_2Nb_2O_6{\cdot}H_2O$ (with $x = 0$), was reported.[15] Surprisingly, in the present study this solid appears as a metastable intermediate in the reaction between Nb_2O_5 and NaOH under hydrothermal conditions and can be achieved by optimizing reaction temperature and time. The synthesis proposed in the present study is relative simple, in terms of both composition and procedures, so that it is highly possible to elucidate the reaction mechanism of the process, which is a part of our effort aimed at comprehensively understanding the general reaction between concentrate NaOH and metal oxides.[25−27,31] By monitoring the structure evolution during the reaction process with various techniques including electron microscopy, X-ray diffraction (XRD), ^{23}Na MAS NMR, and Raman spectroscopy, we are able to deduce the formation mechanism that appears beyond conventional knowledge. This is of notable significance for fundamental research and provides important knowledge for manipulating the chemical reaction process to achieve niobate materials of advanced functions.

II. Experimental Section

1. Sample Preparation. NaOH pellets and Nb_2O_5 (both are AR grade and from Aldrich) were used in the synthesis. In a typical synthesis, 1.0 g of Nb_2O_5 was dispersed in a 60 mL aqueous solution of 10 M NaOH. (*Caution*: Corrosive solutions. Wear gloves in operation and use plastic beaker for NaOH solution and the obtained mixture.) The obtained mixture was autoclaved at a temperature between 100 and 180 °C (hydrothermal reaction) for a period between 30 min and 48 h to yield white niobate solids. The white precipitate in the autoclaved mixture was recovered by centrifugation and washed with deionized water four times by dispersing the wet cake into 100 mL of water and then recovering the solid by centrifugation. In the present study, it was found that at 180 °C the structure evolution of the solid

(10) Nyman, M.; Tripathi, A.; Parise, J. B.; Maxwell, R. S.; Harrison, W. T. A.; Nenoff, T. M. *J. Am. Chem.* Soc. **2001**, *123*, 1529.
(11) Nobre, M. A. L.; Longo, E.; Leite, E. R.; Varela, J. A. *Mater. Lett.* **1996**, *28*, 215.
(12) Nazeri-Eshghi, A.; Kuang, A. X.; Mackenzie, J. D. *J. Mater. Sci.* **1990**, *25*, 3333.
(13) Nyman, M.; Tripathi, A.; Parise, J. B.; Maxwell, R. S.; Nenoff, T. M. *J. Am. Chem. Soc.* **2002**, *124*, 1704.
(14) Xu, H. W.; Nyman, M.; Nenoff, T. M.; Navrotsky, A. *Chem. Mater.* **2004**, *16*, 2034.
(15) Camargo, E. R.; Popa, M.; Kakihana, M. *Chem. Mater.* **2002**, *14*, 2365.
(16) Kormarneni, S.; Roy, R.; Lin, H. C. *Mater. Res. Bull.* **1992**, *27*, 1393.
(17) Uchida, S.; Inoue, Y.; Fujishiro, Y.; Sato, T. *J. Mater. Sci.* **1998**, *33*, 5125.
(18) Liu, J.-F.; Li, X.-L.; Li, Y. D. *J. Cryst. Growth* **2003**, *247*, 419.
(19) Santos, I. C. M. S.; Loureiro, L. H.; Silva, M. F. P.; Cavaleiro, M. V. *Polyhedron* **2002**, *21*, 2009.
(20) Goh, G. K. L.; Lange, F. F.; Haile, S. M.; Levi, C. G. *J. Mater. Res.* **2003**, *18*, 338.
(21) Nowak, I.; Ziolek, M. *Chem. Rev.* **1999**, *99*, 3603.
(22) Cotton, F. A.; Wilkinson, G.; Murillo, C. A.; Bochmann, M. *Advanced Inorganic Chemistry*, 6th ed.; J. Wiley& Sons: New York, 1999; p 897.
(23) Kasuga, T.; Hiramatsu, M.; Hoson, A.; Sekino, T.; Niihara, K. *Adv. Mater.* **1999**, *11*, 1307.
(24) Tian, Z. R.; Voigt, J. A.; Liu, J.; Mckenzie, B.; Xu, H. F. *J. Am. Chem. Soc.* **2003**, *125*, 12384.
(25) Gao, X. P.; Bao, J. L.; Pan, G. L.; Zhu, H. Y.; Wu, F.; Song, D. Y. *J. Phys. Chem. B* **2004**, *108*, 5547.
(26) Zhu, H. Y.; Gao, X. P.; Lan, Y.; Song, D. Y.; Xi, Y. X.; Zhao, J. C. *J. Am. Chem. Soc.* **2004**, *126*, 8380.
(27) Zhu, H. Y.; Lan, Y.; Gao, X. P.; Ringer, S. P.; Zheng, Z. F.; Song, D. Y.; Zhao, J. C. *J. Am. Chem. Soc.* **2005**, *127*, 6730.
(28) Xia, Y.; Yang, P.; Sun, Y.; Wu, Y.; Mayers, B.; Gates, B.; Yin, Y.; Kim, F.; Yan, H. *Adv. Mater.* **2003**, *15*, 353.
(29) Saupe, G. B.; Waraksa, C. C.; Kim, H. N.; Yan, Y. J.; Kaschak, D. M.; Skinner, D. M.; Mallouk, T. E. *Chem. Mater.* **2000**, *12*, 1556.
(30) Du, G. H.; Peng, L.-M.; Chen, Q.; Zhang, S.; Zhou, W. Z. *Appl. Phys. Lett.* **2003**, *83*, 1638.
(31) Gao, X. P.; Lan, Y.; Zhu, H. Y.; Liu, J. W.; Ge, Y. P.; Wu, F.; Song, D. Y. *Electrochem. Solid-State Lett.* **2005**, *8*, A26.
(32) Miyamoto, N.; Nakato, T. *Adv. Mater.* **2002**, *14*, 1267.
(33) Koinuma, M.; Seki, H.; Matsumoto, Y. *J. Electroanal. Chem.* **2002**, *531*, 81.
(34) Kugler, V. M.; Soderlind, F.; Music, D.; Helmersson, U.; Andreasson, J.; Lindback, T. *J. Cryst. Growth* **2004**, *262*, 322.

phase in the reaction system can be clearly observed. Therefore, a series of samples were collected after 30, 60, 80, 100, 120, 140, and 180 min of the hydrothermal reaction, respectively. X-ray fluorescence (XRF) analysis indicated that the washed products possessed a sodium content of ~20 wt % Na_2O, which was sodium niobates, while the sodium content varied from sample to sample. The sodium niobate samples were dried in air at 100 °C. The series of samples obtained at 180 °C are of particular interest in the kinetic control of the product structure and labeled Nb-*n*, where *n* denotes the hydrothermal reaction period (in min). For instance, Nb-*60* is the sample obtained after 60 min of the hydrothermal reaction.

2. Sample Characterization. The morphology and crystal structure of products were investigated using scanning electron microscopy (SEM) and XRD techniques, respectively. The elemental analysis of the samples was conducted by X-ray fluorescence (XRF) on a Philips PW 1480 spectrometer that used a wavelength dispersive technique. The morphology of products was investigated using a Philips XL30 SEM with an accelerating voltage of 10 kV. XRD patterns of the sample powders were recorded using a Siemens D-5000 diffractometer, equipped with a graphite monochromator. Cu Kα radiation ($\lambda = 1.5418$ Å) and a fixed power source (40 kV and 40 mA) were used. The samples were scanned at a rate of 0.12°(2θ)/min over a range of 2−80°, which covers the main characteristic diffraction peaks of the sodium niobates and niobium oxide. The Raman spectra of the samples were measured on a Bruker IFS 100 FT-Raman spectrometer using a 1.5 W Nd:YAG air-cooled laser. All NMR experiments were performed on a Varian/Chemagnetics Infinityplus 400 WB spectrometer operating at a magnetic field strength of 9.4 T. The ^{23}Na resonance frequency at this field strength is 105.7 MHz. A Varian/Chemagnetics T3 4-mm probe was employed to acquire all of the spectra. The ^{23}Na magic angle-spinning (MAS) spectra were acquired by using a conventional one-pulse sequence with a very short rf pulse of 1 μs, which corresponds to a selective 90° pulse (central transition only) of 12 μs. The pulse delay was from 2 to 8 s depending on the sample. The ^{23}Na chemical shifts were referenced to NaCl (aq) by setting the ^{23}Na signal of a solid NaCl sample to $\delta(^{23}\text{Na}) = 7.21$ ppm. The spinning speed was typically at 15 kHz. The ^{23}Na triple quantum magic angle spinning (3QMAS) experiments were performed by using a three-pulse, *z*-filter sequence.[35] The rf strengths of the first two hard pulses and the third soft pulse were individually optimized, and the optimized pulse lengths were 3.7, 1.3, and 10.0 μs for the three consecutive pulses. The spectra were typically obtained using a spinning rate of 15 kHz, a t_1 increment of 22.22 μs, and a total of 128 t_1 increments. 256 scans were acquired with a repetition delay of 8 s for sample Nb-*120* and 2 s for the rest of the samples. All NMR spectra were acquired at room temperature. Simulations of MAS spectra were carried out with the WSOLIDS software package provided by Prof. R. E. Wasylishen (University of Alberta). To investigate the light absorption and emission behaviors of the samples as well as their energy band gap, we measured the diffuse reflectance UV−visible (DR−UV−vis) spectra of the samples on a Varian Cary 5E UV−vis−NIR spectrophotometer and their photoluminescence (PL) spectra on a homemade setup using an Nd:YAG pumped dye laser system (Continuum Powerlight 7010, Lambda Physik LPD3000E, DCM dye, a KDP doubling crystal). The wavelength of the laser as the excitation source at room temperature was 320 nm. Thermogravimetric analysis (TGA) was conducted on a Hi-RES TGA 2950 thermogravimetric analyzer. About 10 mg of dried solid sample was heated from room temperature (about 25 °C) to 700 °C in nitrogen flow of 50 mL/min. High-resolution electron microscopy (HREM) was used to study the detailed structure of niobate fibers (Nb-*120*). HREM was carried out on a FEI F30 TEM operating at 300 kV. To avoid the electron beam damage of the TEM specimen, HREM images were collected digitally with the low-dose model.

(35) Amoureux, J.-P.; Fernandez, C.; Steuernagel, S. *J. Magn. Reson.* **1996**, *A13*, 116.

III. Results and Discussion

3.1. Particle Morphology. The SEM images of the samples in Figure 1 illustrate the interesting morphological evolution of the solid during the hydrothermal reaction at the optimized temperature of 180 °C. The reactant Nb_2O_5 is a fine powder with a particle size of about 100 nm (Figure 1a), and it reacts with the concentrate NaOH solution fast under the hydrothermal conditions, yielding large grains of several micrometers in size in the early stage of the reaction (Figure 1b), and short bar-like particles subsequently (Figure 1c). The bars grew longer as the reaction proceeded, as shown in the micrographs of the Nb-*30*, Nb-*60*, and Nb-*80* samples. Thin wires with length of tens of micrometers and a width of tens of nanometers were then observed in the Nb-*100* sample (Figure 1e). The fibers formed at the expense of the bars and are obviously longer and thinner than the bars. As the reaction proceeded to 120 min, high purity niobate wires were obtained (Figure 1f). Interestingly, the further reaction leads to formation of sodium niobate cubes from the wires, as can be observed in the Nb-*140* sample (Figure 1g). The portion of the cubes in the product increases as the reaction advances until all of the product become cubes (Figure 1h) after 180 min of reaction. Clearly, one can obtain the niobate solid of a desired particle morphology by controlling the reaction time.

3.2. XRD Patterns. As shown in the XRD patterns in Figure 2, after 48 h of hydrothermal reaction at 100 °C, the pattern of the sampled remains the same as that of Nb_2O_5. Yet the patterns of the solids obtained from reaction at 120 °C are profoundly different from that of Nb_2O_5, suggesting that the reaction between NaOH and Nb_2O_5 took place substantially. At 150 °C, the reaction proceeds rapidly. After 3 h, the obtained solid consisted mainly of poorly crystallized niobate.

Another feature of this reaction is the complicated sequence of phase transitions as the reaction advances. This is demonstrated by the XRD patterns of the products obtained from the reaction conducted at 120 °C in Figure 2. Both solids collected after 12 and 24 h are mixtures of residue Nb_2O_5 and at least a niobate. However, there are evidently the diffraction peaks of $Na_7(H_3O)Nb_6O_{19} \cdot 14H_2O$ with an orthorhombic lattice (JCPDS, #84-0188, space group *Pmnn*, $a = 10.072$ Å; $b = 12.148$ Å; $c = 12.722$ Å; $A = 0.8291$ and $C = 1.0473$) in the product obtained after 24 h, while this phase does not exist in the product after 12 h. The major diffractions of this phase are indexed in Figure 2. The framework of such a phase is composed of $Nb_6O_{19}^{8-}$ units, so-called Lindqvist ions,[36] which is a super-octahedron consisting of six edge-sharing NbO_6 octahedra. Nonetheless, there is more than one crystal phase in this sample. It is difficult to achieve pure sample of one crystal phase only. On the other hand, the XRD patterns in Figures 2 and 3 also display complicated phase transitions with changes in the hydrothermal reaction temperature. It seems that the phases appearing in the reaction system are very sensitive to the reaction conditions and kinetic dependent. Under such circumstances, the reaction temperature must be carefully optimized and the reaction kinetics controlled to yield the products of a desired crystal phase and high purity.

The XRD patterns of the solids sampled after various periods of the reaction at 180 °C are presented in Figure 3, which indicate pronounced changes in crystal structure during the course of the reaction.

(36) Lindqvist, I. *Ark. Kemi* **1953**, *5*, 247.

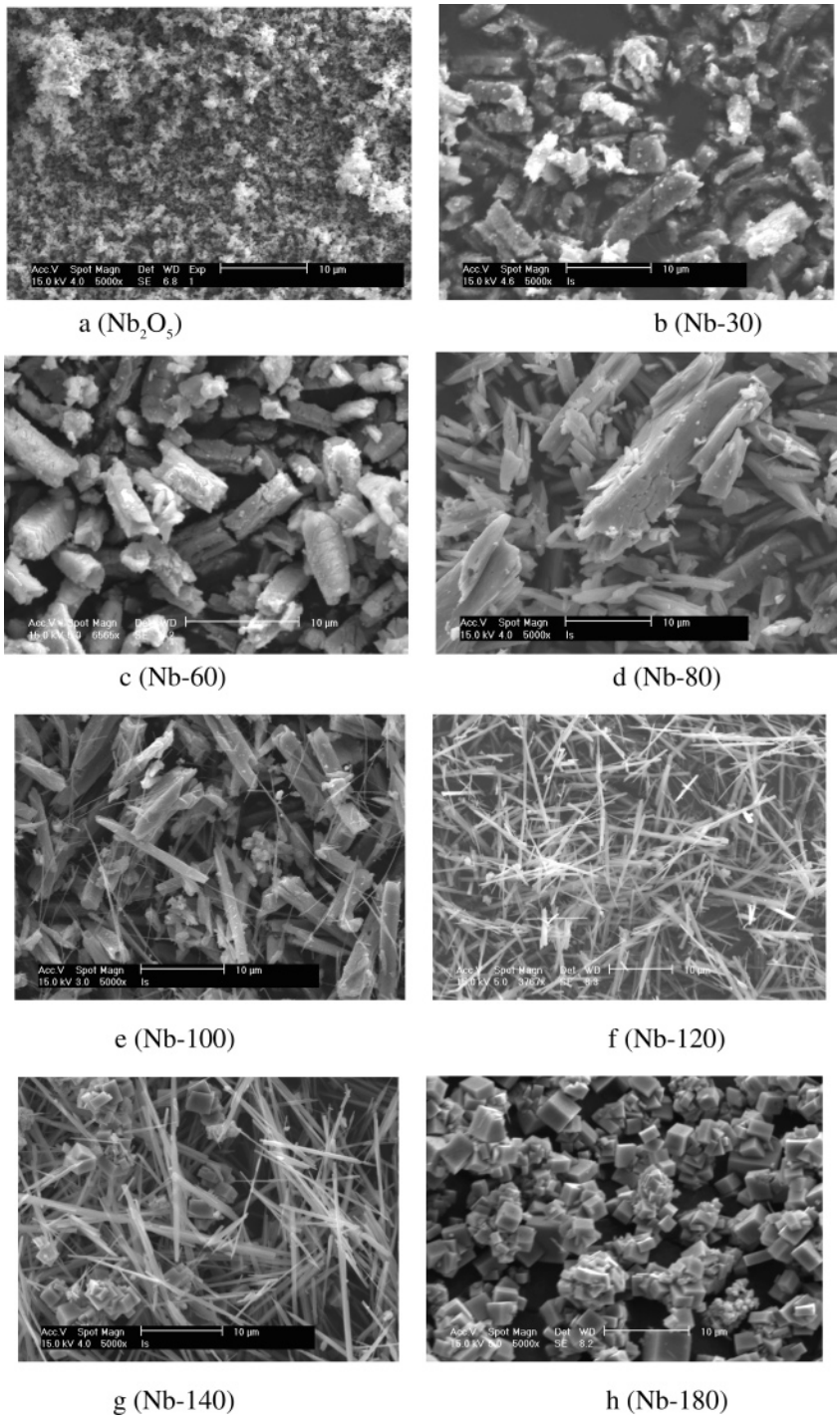

Figure 1. The morphological evolution of the niobate solid during the reaction course illustrated by SEM images of the samples: (a) the starting Nb_2O_5 powder, (b) Nb-*30*, (c) Nb-*60*, (d) Nb-*80*, (e) Nb-*100*, (f) Nb-*120*, (g) Nb-*140*, and (h) Nb-*180*.

The patterns of the Nb-*30* and Nb-*60* samples are distinctly different from that of the starting Nb_2O_5, indicating that new crystal phase forms at the expense of Nb_2O_5 in a short period. It is known that niobium pentoxide powder dissolves in the concentrated caustic soda.[15] The new phase of the large particles observed in SEM images should be a sodium niobate, which coexists with the unreacted Nb_2O_5. The diffraction peaks of the latter are still observed in Nb-*30* and Nb-*60*, suggesting that they are mixtures containing more than one phase. Nevertheless, this niobate phase appears as a metastable intermediate, and its crystallinity degrades readily in the subsequent reaction process. The reflection peaks in the XRD patterns of the Nb-*80* and Nb-*100* are broad and have low intensity, indicating poor crystallinities in these bar-like solids. Surprisingly, well-crystallized fibers form from the poorly crystallized solids with a relative irregular shape in the subsequent short period of only 20 min. The fibers are of particular interest because of their crystal and morphological features. The Na:Nb ratio of the fibers is near 1 (1.04), and the XRD pattern of the fibers is similar to that of the microporous molecular sieves, SOMS, with a formula of

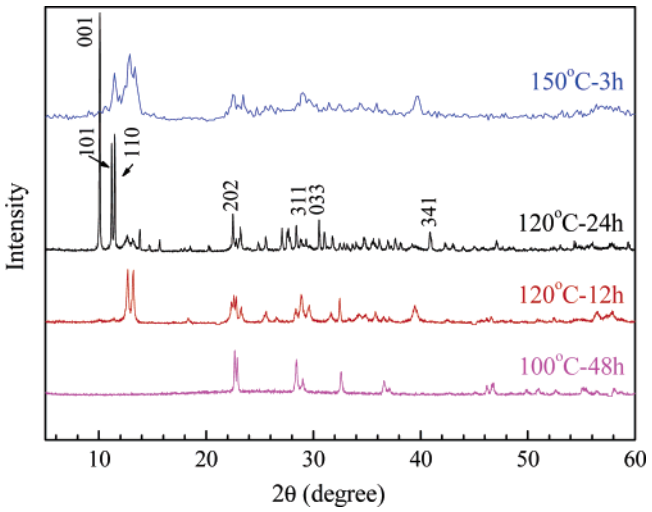

Figure 2. XRD patterns of the solids sampled prepared at temperatures between 100 and 150 °C.

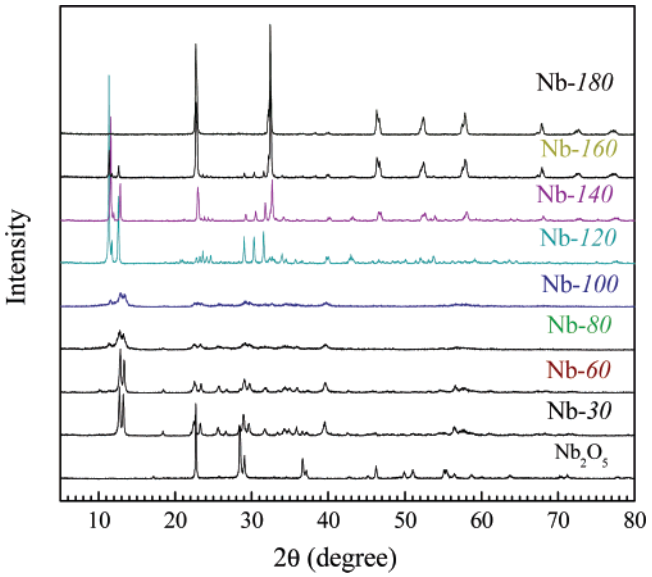

Figure 3. The XRD patterns of the solids sampled after various reaction periods (which are indicated in the figure). The patterns show the phase transitions during the reaction course at 180 °C.

$Na_2Nb_{1-x}Ti_xO_6(OH)_x \cdot H_2O$.[37] To clarify the crystal structure of the fibers, we fit the XRD data with the Rietveld method using the program RIETICA.[38]

The starting structural parameters were taken from the recent work of Xu et al.[14] (space group $C2/c$, $a = 17.0511$ Å; $b = 5.0293$ Å; $c = 16.4921$ Å; $\beta = 113.942°$), and the calculated pattern fit well with the measured data when the crystal parameters were space group $C2/c$, $a = 17.0546(5)$ Å; $b = 5.0293(2)$ Å; $c = 16.5447(7)$ Å; $\beta = 113.907°$. Meanwhile, the major diffraction peaks of the fibers are also indexed according to the Rietveld refinement, as shown in Figure 4.

These results indicate that there is only one niobate crystal phase of a monoclinic lattice in the fibril solid of Nb-*120*. Nevertheless, this phase appears to be a metastable crystal phase. New peaks are observed in the patterns of the samples after

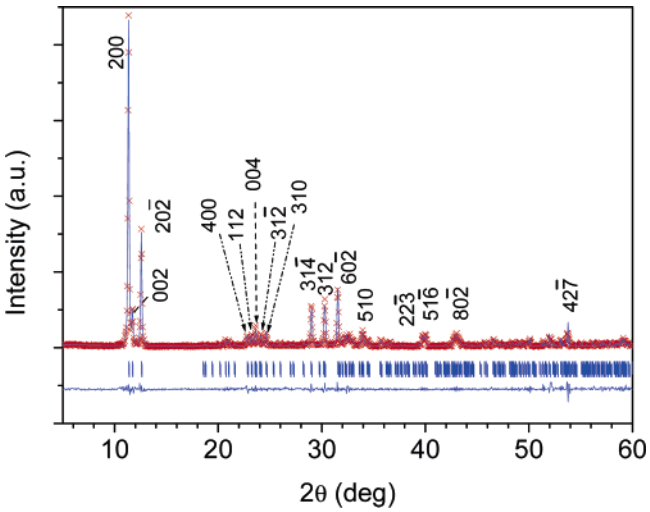

Figure 4. Fitted XRD pattern of the niobate fibers. The plus signs denote the measured XRD data, and the solid curve is the best fit to the data. The vertical bar marks below the pattern show the positions of allowed reflections, and the lower curve represents the difference between the observed and calculated profiles.

Table 1. Na:Nb Ratio and the Possible Formula of the Sodium Niobates

sample	Na/Nb ratio	possible formula
Nb-*60*	1.18	$Na_{8-x}(H_3O)_xNb_6O_{19} \cdot nH_2O$ and Nb_2O_5
Nb-*120*	1.04	$Na_2Nb_2O_6 \cdot {}^2/_3H_2O$
Nb-*180*	1.05	$NaNbO_3$
Nb-*120*-Li	0.59	$Na_{1.2}Li_{0.8}Nb_2O_6 \cdot {}^2/_3H_2O$

140 min of reaction, which are from a coexistent phase; meanwhile, the relative intensity of the peaks from the fibers weakens. The new phase formed after 140 min should be the cubes shown in the SEM images, and they form at the expense of fibers. The Nb-*180* sample is pure cuboids, as shown in Figure 1h, and the appearance of its XRD pattern suggests that there probably is only one crystal phase in this sample. The Na:Nb ratio of the sample is also about 1 (1.05), and the possible formula for the Nb-*180* sample is $NaNbO_3$. There are a number of $NaNbO_3$ polymorphs that can crystallize at ambient temperatures, including orthorhombic, tetragonal, and monoclinic.[39,40] We found that all peaks in the XRD pattern of Nb-*180* are best fitted with those for the tetragonal lattice (*P*4/*mbm*) when the refinement started with the parameters in JCPDS Card # 73-1106, and the lattice parameters $a = 5.516(1)$ Å, $c = 3.944$ (1) Å. The Nb-*180* is stable $NaNbO_3$ crystalline, in terms of the crystal phase, morphology, and Na:Nb ratio. These properties remain unchanged when the reaction was prolonged to 48 h.

3.3. Composition and Ion Exchange Ability of the Niobates. The Na:Nb ratios of the niobate samples, calculated from XRF results, are given in Table 1. The ratio varies as the reaction proceeds and approaches unity for the final product of $NaNbO_3$. The possible formulas of the niobate samples can be given based on the ratio. For instance, the Na:Nb ratio of the sample after 60 min of reaction, Nb-*60*, is 1.18, calculated from the XRF analysis results. Because the sodium niobate phase, $Na_{8-x}(H_3O)_x$-$Nb_6O_{19} \cdot nH_2O$, was found in the product of the reaction at 120 °C for 24 h (Figure 2), Nb-*60* sample is probably a mixture of

(37) Iliev, M. N.; Phillips, M. L. F.; Meen, J. K.; Nenoff, T. M. *J. Phys. Chem. B* **2003**, *107*, 14261.
(38) Howard, C. J.; Hunter, B. A. *A Computer Program for Rietveld Analysis of X-ray and Neutron Powder Diffraction Patterns*; Lucas Heights Research Laboratories: Sydney, 1988; pp 1−27.
(39) Lanfredi, S.; Dessemond, L.; Martins, A. C. *J. Eur. Ceram. Soc.* **2000**, *20*, 983.
(40) Darlington, C. N. W.; Knight, K. S. *Physica B* **1999**, *266*, 368.

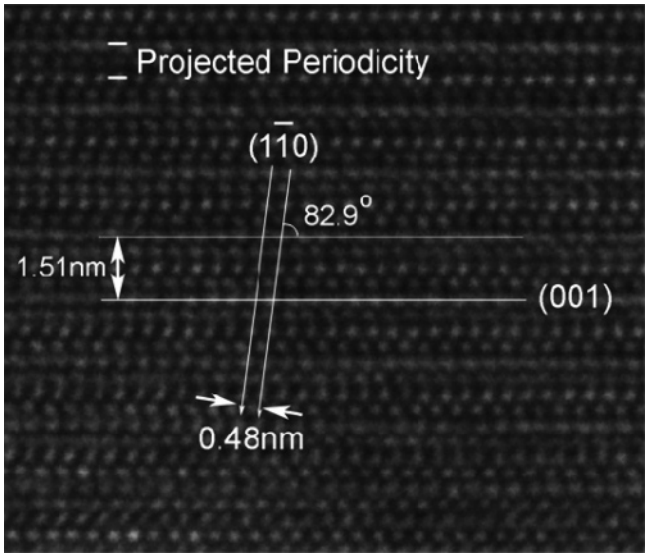

Figure 5. [110] HREM image of the fibril niobate $Na_2Nb_2O_6 \cdot {}^2/_3H_2O$.

$Na_{8-x}(H_3O)_xNb_6O_{19} \cdot nH_2O$ and Nb_2O_5. Because the fibers are the single-crystal phase of greatest interest, thermogravimetric analysis (TGA) of the sample was conducted in air from room temperature (~25 °C) to 600 °C. The largest weight loss appears between 250 and 400 °C, about 3.34%. From this weight loss, the number of water molecules in the possible formula in Table 1 is about two-thirds (0.63). Therefore, the formula for Nb-*120* is $Na_2Nb_2O_6 \cdot {}^2/_3H_2O$.

Lithium niobate is a well-known nonlinear optical material, which is widely used for various purposes.[3] Moreover, introducing lithium into sodium niobate, even in small amounts, produces new materials with unique properties that are of practical importance. The properties include high sound speed, a wide range of Curie temperatures and dielectric constants, as well as piezoelectric characteristics.[4,41−42] In the present study, introducing lithium into the niobate fibers by an ion exchange process was conducted. The Nb-*120* niobate fibers were dispersed into a solution of 0.1 M LiCl to exchange the Na^+ ions in the fibers with Li^+ ion at room temperature. The sample so obtained is labeled Nb-*120*-Li. As shown in Table 1, over 40% of sodium in the Nb-*120* has been exchanged. This approach that we used is viable for preparing lithium/sodium niobate functional materials. Two interesting facts are noted: first, only part of the Na^+ ions in the fiber is exchanged with Li^+ ions. Second, the ion exchange experiment was also carried out with Nb-*180*, but Na^+ ions in the $NaNbO_3$ cubes could not exchange with the Li^+ ions in solution. This solid has no micropores in which exchangeable sodium ions may exist.[39,40]

3.4. HRTEM. To determine the detailed structure of niobate fibers, HREM was used. Figure 5 shows a typical HREM image taken from the [110] zone axis. As can be seen clearly from the HREM images, the hydrothermal synthesized fibers are well-crystallized. The fact that (1) the distance between two neighboring (1$\bar{1}$0) atomic planes is 0.48 nm, (2) the distance between two neighboring (001) atomic planes is 1.51 nm, and (3) the angle between {1$\bar{1}$0} planes and {001} planes is 82.9° proved that the niobate fibers have the lattice parameters determined by refined XRD results. Upon further analysis of Figure 5, it can be seen that, although there are four molecular layers within two neighboring (001) atomic planes, the alternation of a brighter dotted layer and a weaker dotted layer indicates the projected periodicity of the crystal structure along the [110] direction containing only two molecular layers. This is consistent with the *C*2/*c* space group of niobate fibers.

3.5. Solid-State ^{23}Na NMR. Solid-state ^{23}Na NMR spectroscopy was also used to probe the development of local environments of the sodium ions within different phases as a function of reaction time because ^{23}Na NMR parameters are sensitive to the local electronic structure and the coordination geometry. The selected ^{23}Na MAS spectra of the samples collected during the reaction are shown in Figure 6. The simulated spectra of some samples are also given in the figure, providing further information of the different sodium sites in the solids.

The spectra of the sample heated for 30 and 60 min (Nb-*30*, Nb-*60*) both exhibit a rather broad asymmetric envelope with the maximum at around 2 ppm. After 80 min of heating, a new high-field resonance started appearing at −8 ppm. Heating the sample for 100 min resulted in significant line broadening; the spectrum of sample Nb-100 contains at least two broad overlapping resonances. Overall, for the samples heated for less than 120 min, the broad signals with ill-defined line shape are quite similar to those observed for amorphous or disordered materials, [43,44] indicating the distribution of chemical shift and/or quadrupole-induced shift. Heating the sample for 120 min yielded a distinctly different ^{23}Na MAS spectrum. The spectrum looked identical to that of $Na_2Nb_2O_6 \cdot H_2O$ reported by Xu et al.,[14] further confirming the finding from XRD that sample Nb-*120* is $Na_2Nb_2O_6 \cdot {}^2/_3H_2O$. The line shape of ^{23}Na signals continues to change with increasing reaction time. It eventually evolved into a distinct new pattern after 180 min of heating time. Further increasing the reaction time to 48 h did not result in a noticeable change in the spectrum.

The appearance of the MAS spectra clearly indicates that, for each sample, there are at least two and even more sodium sites. However, in most cases, they are not resolved. The low-resolution of ^{23}Na MAS NMR is due to the fact that, as a quadrupolar nucleus, ^{23}Na ($I = {}^3/_2$) experiences a quadrupolar interaction of the nuclear quadrupolar moment (eQ) with the electric field gradient (eq), which is characterized by the quadrupolar coupling constant, $C_q = e^2qQ/h$, and asymmetry, η, where $0 \leq \eta \leq 1$. The second-order quadrupolar interaction cannot be completely averaged out by spinning the sample at magic angle. Recently, the multiple quantum magic-spinning (MQMAS) method has been developed,[45] which can effectively eliminate the second-order quadrupolar interaction experienced by half-integer quadrupolar nuclei, and thus narrow the asymmetric line shape considerably. This two-dimensional technique allows one to obtain isotropic (high-resolution) spectra on F_1 dimension and the separation of the overlapping second-order broadened patterns along the F_2 dimension. To determine the number of overlapping resonances due to different sites for each sample, we measured ^{23}Na triple quantum magic-spinning

(41) Nitta, Pozdnyakova, I.; Navrotsky, A. *J. Am. Ceram. Soc.* **2002**, *85*, 379.
(42) Zeyfang, R. R.; Henson, R. M.; Maier, W. J. *J. Appl. Phys.* **1977**, *48*, 3014.
(43) Antonijevic, S.; Ashbrook, S. E.; Walton, R. I.; Wimperis, S. *J. Mater. Chem.* **2002**, *12*, 1469.
(44) Hwang, S.-J.; Fernandez, C.; Amoureux, J. P.; Han, J.-W.; Cho, J.; Martin, S. W.; Pruski, M. *J. Am. Chem. Soc.* **1998**, *120*, 7337.
(45) Frydman, L.; Harwood, J. S. *J. Am. Chem. Soc.* **1995**, *117*, 5367.

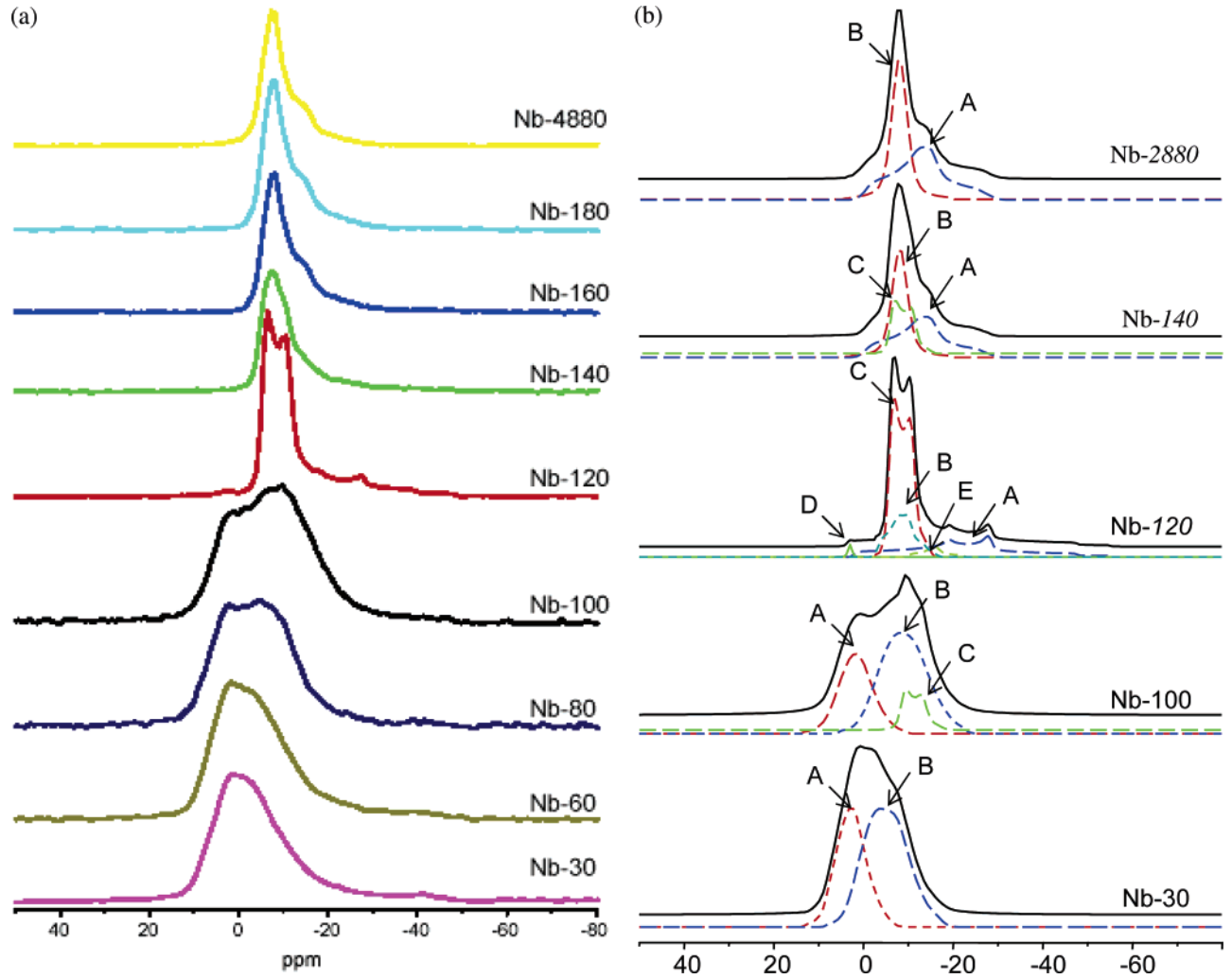

Figure 6. The ^{23}Na MAS spectra of the samples collected during the reaction: (a) the measured spectra of the samples; (b) the simulated spectra of some samples in panel (a).

Table 2. ^{23}Na NMR Parameters for Selected Na Sites

sample	site	$\delta_{iso,3Q}$/ppm	P_q/MHz	$\delta_{iso}{}^{CS}$/ppm	C_q/MHz	η
Nb-*30*	A	10	1.6	8		
	B	4	2.0	3	1.9	0.5
Nb-*100*	A	10	1.6	7		
	B	4	2.0	−1	1.9	0.5
	C	−5	1.4	−8	1.4	0.1
Nb-*120*	A	3	3.3	3	3.1	0.7
	B	−3	1.7	−3	1.5	0.6
	C	−5	1.4	−5	1.4	0.1
Nb-*140*	A	0	2.4	0	2.2	0.8
	B	−7	0.5	−8	0.5	0.5
	C	−5	1.4	−5	1.4	0.1
Nb-*2880*	A	0	2.4	0	2.2	0.8
	B	−7	0.5	−8	0.5	0.5

(3QMAS) spectra. Figure 7 illustrates the 3QMAS spectra of selected samples.

For each sample, from the observed isotropic shift in F_1 dimension ($\delta_{iso,3Q}$) and the F_2 cross-section sub-spectra, the ^{23}Na NMR parameters [C_q, η, isotropic chemical shift ($\delta_{iso}{}^{CS}$), and the "second-order quadrupole" parameter (SOQE): $P_q = C_q(1 + \eta^2/3)^{1/2}$] for individual sites were extracted (Table 2), and 1D ^{23}Na MAS spectra were simulated (Figure 6b). For sample Nb-*30*, the 3QMAS (Figure 7a) and simulated MAS spectra (Figure 6b) clearly indicate that there are two sodium sites. For resonance A, the sheared spectrum exhibits a tilted signal along the axis of chemical shift distribution, suggesting that there is a range of δ_{iso} values with a roughly constant C_q for this site.[46] The XRD pattern of this sample indicates that the sample is a mixture of unreacted Nb_2O_5 and a sodium niobate. Although a formula was proposed for this sodium niobate based on chemical analysis (Table 1), the actual structure is not known. Our ^{23}Na NMR data provide some information on the Na^+ ions in the structure. Becayse Nb_2O_5 has no sodium ions, the ^{23}Na signals observed must originate solely from the new sodium niobate. Thus, the NMR results show that this sodium niobate has two distinct sodium sites with one site (resonance A) being disordered and the other (resonance B) having a relatively asymmetric environment indicated by a relatively large C_q. The MAS spectrum of sample Nb-*100* exhibits a broad profile with two overlapping signals. The corresponding 3QMAS spectrum (Figure 7b) illustrates unambiguously that, in addition to the two sites (signals A and B) observed in sample Nb-*30*, a new site (signal C) appears, and the appearance of the new site signalizes the formation of a new phase, and we do observe a few thin fibers in this sample (Figure 1e).

(46) Bodert, P. R. *J. Magn. Reson.* **1998**, *133*, 207.

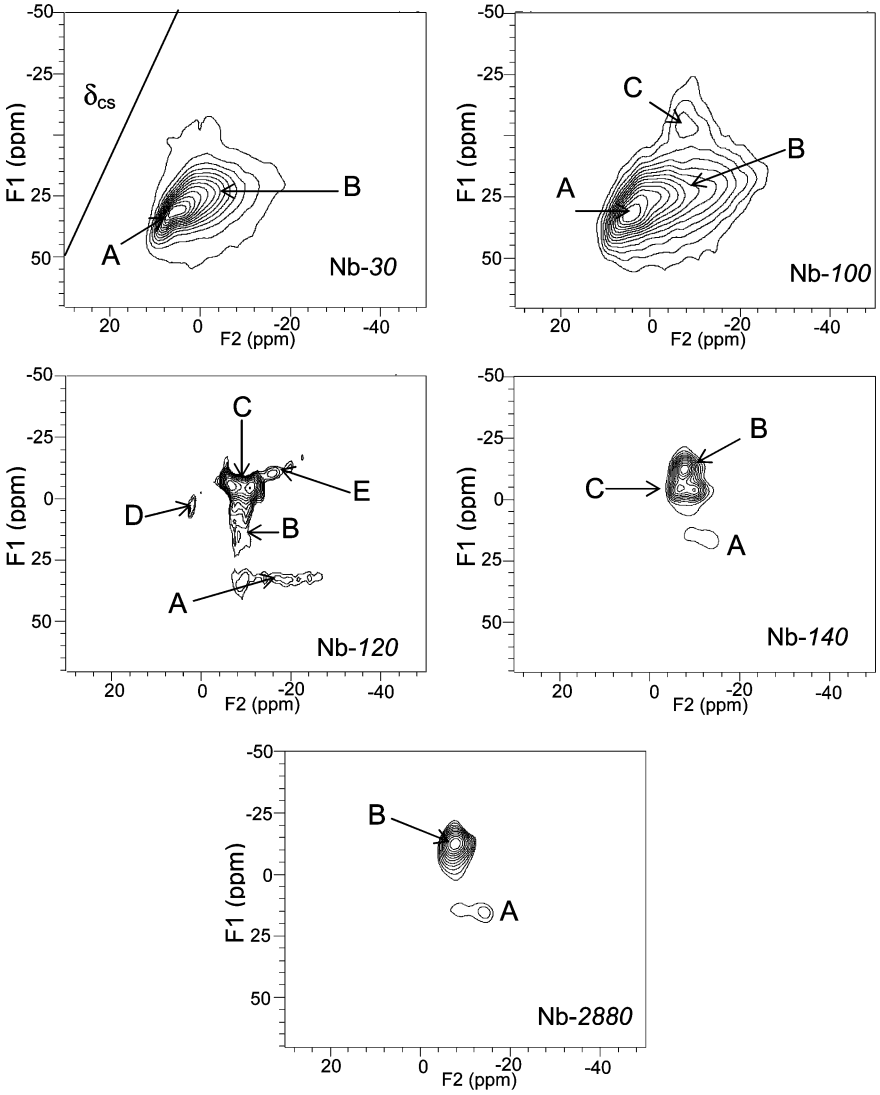

Figure 7. The 3QMAS spectra of selected samples: (a) Nb-*30*, (b) Nb-*100*, (c) Nb-*120*, (d) Nb-*140*, and (e) Nb-*2880*.

Sample Nb-*120* is a high-purity crystalline phase according to the XRD pattern, and its 3QMAS spectrum reveals five signals. Two extremely weak signals (D and E) are likely due to either the residual sodium niobate phase found in sample Nb-*30* or a very small amount of impurity. The three major resonances (A, B, and C) belong to the new phase of $Na_2Nb_2O_6 \cdot {}^2/_3H_2O$. The slices taken through signals A, B, and C exhibit distinct quadrupolar powder patterns with different C_q and η values (Table 2). The powder synchrotron XRD refinement suggests that there are three Na sites: Na(1) and Na(2) are part of the framework, and Na(3) is an extraframework ion.[14] The occupancies for Na(1):Na(2):Na(3) are 1:0.5:0.5. On the basis of the XRD data, we were able to assign the observed ^{23}Na NMR signals to the appropriate Na sites in the structure. The extraframework Na [Na(3)] is coordinated to four oxygen atoms in a distorted square plan with a Na−O distance variation of 2.12−2.43 Å, and a fifth capping oxygen is 2.84 Å from Na-(3). Because such a low local-symmetry should result in a large C_q, we assign the resonance A with a very large C_q of 3.1 MHz to Na(3). The remaining two signals, B (C_q, 1.6 MHz) and C (C_q, 1.4 MHz), are due to Na(1)O_6 and Na(2)O_6 octahedra present in the framework. Structural data show that Na(1) is bonded to five framework oxygen atoms and one water oxygen and Na(2) is coordinated to six framework oxygen atoms.[13,14] The variation of the Na−O distance is 2.33−2.64 and 2.33−2.76 Å for Na(1) and Na(2), respectively. The irregularity of these octahedra explains the relatively large C_q values for a Na in an octahedral geometry. Taking into consideration the difference in C_q values and the population ratio of Na(1):Na-(2), we tentatively assign resonances C and B to Na(1) and Na-(2), respectively. Na(1) is clearly seen in the sample Nb-*100*, which indicates that this particular framework Na site is formed in the early stages of the crystallization.

The 3QMAS and simulated MAS spectra of sample Nb-*140* illustrate that there are three distinct signals. Resonance C is due to $Na_2Nb_2O_6 \cdot {}^2/_3H_2O$. The appearance of two new signals (A and B) confirms the result obtained from XRD that a new phase ($NaNbO_3$) starts forming after heating the reaction mixture for 140 min. The 3QMAS spectrum of Nb-*2880* shows clearly that there are two Na sites in $NaNbO_3$. These sites have very different local environments. Resonance B has a fairly small C_q value of 0.7 MHz, apparently resulting from a rather high local-symmetry at this site. The C_q value (2.3 MHz) of the other Na site (signal A) is, however, quite large. The large C_q indicates a low symmetry environment at this Na site. The crystal

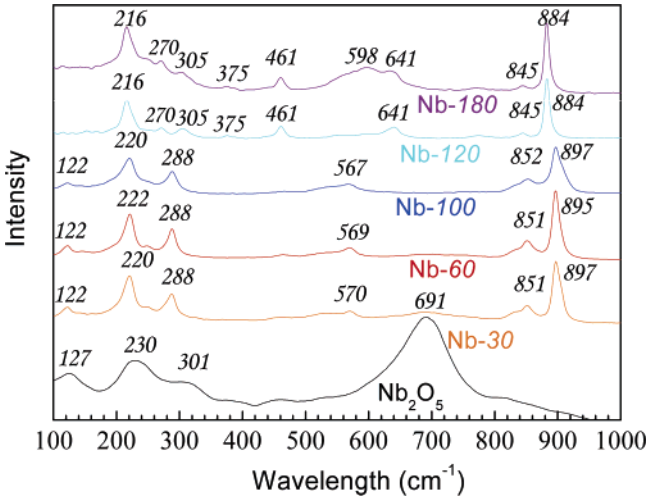

Figure 8. Raman spectra of the reactant Nb_2O_5 and niobate products.

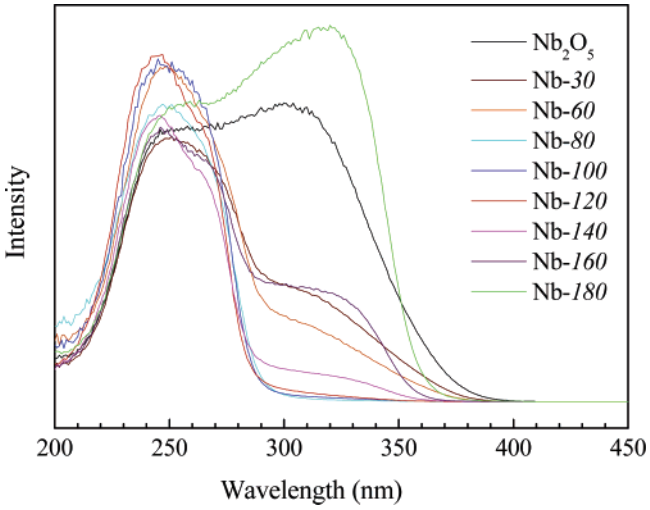

Figure 9. The DR−UV−vis spectra of the reactant Nb_2O_5 and niobate products.

structure of $NaNbO_3$ at ambient conditions[47] shows that there are two independent Na^+ ions with very different environments: Na(1) has three nearest oxygen neighbors in a triangle. Na(2) is in the center of a tetrahedron with 4 oxygen neighbors, an environment with a much higher symmetry. Thus, we assign unambiguously the resonance A to Na(1) and signal B to Na-(2). The NMR data are in excellent agreement with those of single-crystal X-ray diffraction.

3.6. Raman Spectra. The vibrations related to specific polyhedral structures of niobium and oxygen can be discriminated with Raman spectra.[37,39,48−51] The Raman spectra of the samples are illustrated in Figure 8. There have been a number of reports on the Raman spectra of niobate,[5,51] octahedral oxyanions $Nb_6O_{19}^{8-}$ in aqueous solution,[50] niobium oxide in various forms,[48,49,51] and SOMS.[37] The band positions of the Raman spectra provide important structural information of the samples.

For starting material Nb_2O_5, the major band is at 690 cm^{-1} (Figure 8, the lowest trace), which is the characteristic band for the structure consisting of NbO_6 octahedra-sharing corners,[52] and the Nb_2O_5 spectrum is consistent with that reported in the literature.[48] The 690 cm^{-1} band is absent in spectra of the niobate products, indicating that the reaction with NaOH ruptures the corner-sharing between Nb−O polyhedra in Nb_2O_5 crystalline. At 180 °C, the corner-sharing has been broken within a period as short as 30 min, causing radical structural changes. It is noted that in Figure 8 the spectra of some niobates possess the spectral features of oxyanions consisting of NbO_6 octahedra, such as $Nb_6O_{19}^{8-}$ species in solution,[19,50] or hydrated niobium oxide monolayer.[48,49] There is a strong band in the 884−897 cm^{-1} region for all of the niobate samples, and this band should arise from the short Nb═O stretching mode (A_{1g}),[48,50] The bands at 845−851 cm^{-1} are also due to the vibration of the short Nb═O bond (∼1.8 Å),[37,50] and the band at 567−570 can be assigned to the Nb−O−Nb stretching mode (E_g). A band at 461 cm^{-1} is observed for these two samples, which also appears in the spectra for $Nb_6O_{19}^{8-}$ species in aqueous solution and was assigned to the bridge M−O stretching mode with T_{2g} symmetry. The bands at about 290 and 220 cm^{-1} arise from the breathing vibration of the long Nb−O bonds and Nb−O−Nb (bridging O atom) bending mode (A_{1g} and T_{2g}, respectively).[50] The A_{1g} band observed at 288 cm^{-1} in the spectra of the product collected in early stages splits into two weak bands at 270 and 305 cm^{-1}, respectively, in the well-crystallized Nb-*120* and Nb-*180* samples. The reason of the split is not clear yet in this stage. The band at 641 cm^{-1} observed for these two samples is the major difference in the spectra between these two samples and other niobates collected in early reaction stages. This band is much broader and stronger in the spectrum of Nb-*180* than that in the spectrum of Nb-*120*. This band is probably associated with corner-sharing of NbO_6 octahedra, which began re-forming as the reaction proceeds. In the product niobates collected in early reaction stages, NbO_6 octahedra share edges with other octahedra, while in well-crystallized Nb-*120*, the corner-sharing of NbO_6 octahedra occurs, and in Nb-*180* the corner-sharing NbO_6 octahedra are the major structure feature. Actually, the Raman spectrum of the fibril sample Nb-*120* is very similar to that of SOMS,[37] further confirming that the Nb-*120* are microporus solids of the same structure of SOMS.

Raman spectra reflect different structural information from XRD, which are sensitive to the local atomic-site coordination.[48−51] The spectra of the intermediates from Nb-*30* to Nb-*100* have a similar appearance, but the XRD patterns of these samples are remarkably different. The major bands in these spectra are due to edge-sharing NbO_6 octahedra. However, the NbO_6 octahedra can arrange into a variety of crystals by edge-sharing, leading to different XRD patterns.

3.7. UV−Visible Absorption. The UV−vis spectra of the samples are illustrated in Figure 9. The UV−vis absorption reflects the gap between the valence band and conductive band of niobates and niobium oxide, and the band gap is affected by the configuration of NbO_6 octahedra, or coordination symmetry of metal atoms in these solids.[52,53] As anticipated, the structural evolution illustrated above is accompanied by remarkable changes in the optical properties of the solid.

There appear two major absorption bands for Nb_2O_5 with maxima at about 245 and 320 nm (Figure 9), respectively. The

(47) Sakowski-Cowley, A. C.; Lukaszewicz, K.; Megaw, H. D. *Acta Crystallogr., Sect. B* **1969**, *25*, 851.
(48) Jehng, J. M.; Wachs, I. E. *Catal. Today* **1990**, *8*, 37.
(49) Jehng, J. M.; Wachs, I. E. *J. Phys. Chem.* **1991**, *95*, 7373.
(50) Farrell, F. J.; Maroni, V. A.; Spiro, T. G. *Inorg. Chem.* **1969**, *8*, 2638.
(51) Morosin, B.; Peercy, P. S. *Chem. Phys. Lett.* **1976**, *40*, 263.
(52) Blasse, G.; Van den Heuvel, G. P. M. *Mater. Res. Bull.* **1972**, *7*, 1041.
(53) Blasse, G. *Struct. Bond.* **1980**, *42*, 1.

Scheme 1. Structure Evolution during the Reaction Course[a]

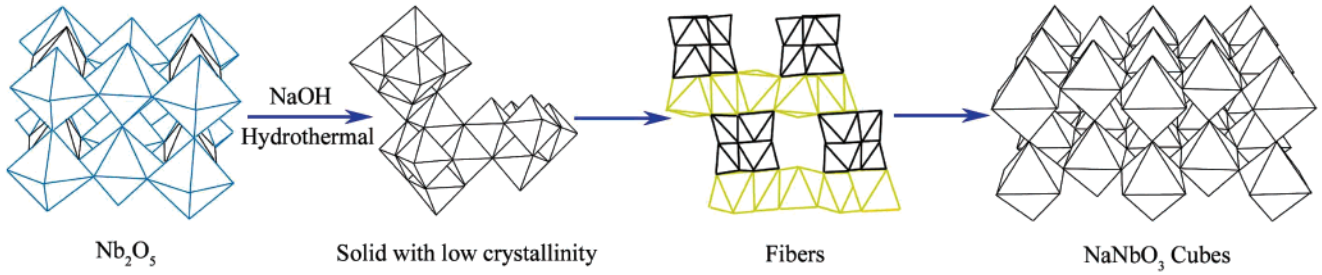

[a] In the Nb_2O_3 structure, NbO_7 decahedra are in bright blue and NbO_6 octahedra are in dark blue. In the microporous fibers, NaO_6 octahedra are in yellow. Na^+ cations locate in the space between NbO_6 octahedra and NaO_6 octahedra.

reaction between Nb_2O_5 and NaOH resulted in pronounced changes in the UV−vis spectra of the products. In bulk crystal structures, the NbO_6 octahedra link each other by corner-sharing, forming three-dimensional lattices, and a large fraction of Nb atoms are in positions with a coordination of high symmetry. According to Blasse and co-workers,[52−55] the band gap of the corner-sharing NbO_6 octahedra in which the Nb atom in the positions with high coordination symmetry is 3.5 eV, corresponding to the absorption band at ~320 nm, while the band at ~250 nm is from the NbO_6 octahedra with other configurations, for instance, edge-sharing octahedra. In such a configuration, the Nb−O distance in one octahedron could be different (distorted NbO_6 octahedra), and thus the coordination symmetry of Nb atoms in these structures is lower. As the reaction advances, the intensity of the absorption at 320 nm decreases markedly. This could be explained as the reaction gradually breaking the corner-sharing of NbO_7 decahedra and NbO_6 octahedra in starting Nb_2O_5. The sample obtained after 80 min of reaction, Nb-*80* and Nb-*100* samples, do not absorb light with wavelength above 300 nm, suggesting that the corner-sharing of NbO_6 octahedra has finally completely broken down. The two samples are also poorly crystallized solids (Figure 3), which could not retain the arrays of corner-sharing NbO_6 octahedra. Nb-*120* sample has a weak but observable light absorption above 300 nm. As demonstrated by the results of XRD, NMR, and Raman spectra, the Nb-*120* sample consists of well-crystallized fibers so that a new configuration of the NbO_6 octahedra has formed, in which the NbO_6 octahedra are in an ordered arrangement, and the corner-sharing is not an important mode by which the NbO_6 octahedra join to each other. As the cubic $NaNbO_3$ crystals appear (Figure 1g), the absorption at about 300 nm increases remarkably (Figure 9, the spectrum of the Nb-*140* sample). This absorption enhances along with the increasing fraction of the $NaNbO_3$ crystals. In the spectrum of the Nb-*180* sample, the intensity of this absorption is much higher than that of the absorption at 245 nm, and the peak shifts to 320 nm. Indeed, the NbO_6 octahedra in $NaNbO_3$ crystals join together by corner-sharing according to ref 56 (the structure is also shown later in Scheme 1). Besides, the Nb-*120* fibers absorb mainly the irradiation with wavelength <300 nm so that they are able to filter the UV irradiation with such wavelength out and reflect the UV light with longer wavelength (>300 nm).

IV. Discussion

4.1. Reactivity of Niobium Pentoxide in Hydrothermal Process. In contrast to the conventional knowledge,[21,22] our study shows that Nb_2O_5 reacts with concentrated NaOH solution at temperatures as low as 120 °C. This reaction temperature is substantially lower than those reported in the literature,[16−18,20] so that the reactivity is surprisingly high and there are numerous products of various structures, depending on the temperature and time of the reaction as shown in Figures 1−3.

The wet-chemical reaction at low temperature for the synthesis of metal oxides and polyoxometalates has unique merits.[57] It is impossible to yield niobate fibers with a high purity by the conventional solid-state synthesis route using sodium carbonate and Nb_2O_5 and the hydrothermal reactions at high temperatures (200 °C or above). Besides, the product niobate fibers and cubes have a homogeneous composition, crystallization, and morphology, which are difficult to achieve by the solid-state reaction route because high sintering temperatures often cause serious volatilization of the alkali metal, which leads to stoichiometric variations in the sintered material.[39] The unexpected high reactivity of the hydrothermal reaction and the metastability of the $Na_2Nb_2O_6 \cdot {}^2/_3H_2O$ phase are probably the main reasons that these fibers of a high purity were not synthesized previously by the direct reaction between Nb_2O_5 and NaOH. Generally, such reactions were carried out for hours or even days.[10,13,14,16−20] Yet, in the reaction at 200 °C or above, one cannot observe fibers after 1 h of reaction, and it is extremely difficult to observe pure fibers in the early stage of the reaction. There is only a small window for such opportunity in the reaction, and careful optimization of the reaction temperature and time is required to achieve high-purity fibers with such a delicate structure. The optimal combination of the reaction temperature and time is at 180 °C for 120 min. With the optimized reaction temperature and time determined, the synthesis in this study is obviously superior to the reported methods for SOMS synthesis, in particular, for the large-scale production of this material.[58]

4.2. The Reaction Mechanism. Recently, there have been different proposals on the reactions involved in the synthesis of potassium niobates under hydrothermal conditions.[18,20] Potassium niobates have attracted more attention because they are ferroelectric at room temperature. In these reports, the reactions were described mainly as that Nb_2O_5 reacted with OH^- and K^+ ions are not often involved. The synthesis reaction in the

(54) Blasse, G.; Van den Heuvel, G. P. M. *Mater. Phys. Chem*. **1986**, *14*, 481.
(55) Wiegel, M.; Hamoumi, M.; Blasse, G. *Mater. Chem. Phys*. **1994**, *36*, 289.
(56) Xu, H. W.; Navrotsky, A.; Su, Y.; Balmer, M. L. *Chem. Mater*. **2005**, *17*, 1880.
(57) Dias, A.; Ciminelli, V. S. T. *Chem. Mater*. **2003**, *15*, 1344.
(58) Nenoff, T. M.; Pless, J. D.; Michaels, E.; Phillips, M. L. F. *Chem. Mater*. **2005**, *17*, 950.

current study also mainly involves Nb_2O_5 and OH^-, so that there could be common features in the reaction mechanism in this study and those proposed in the literature. According to the results of UV−vis spectra (Figure 9), the reaction initially ruptures the corner-sharing of niobium−oxygen polyhedra (decahedra and octahedra, see Scheme 1) in the reactant Nb_2O_5, yielding intermediates with edge-sharing octahedra. In the corner-sharing mode (Nb−O−Nb), the distance between Nb and O atoms is longer than that in the edge-sharing mode.[59] It is reasonable that concentrated NaOH ruptures the corner-sharing. The intermediates could possess a poor crystallinity due to the rupture as shown in Nb-*80*. Therefore, the first step reaction is rupturing the corner-sharing between NbO_6 octahedra:

$$Nb_2O_5 + 8OH^- \rightarrow Nb_6O_{19}{}^{8-} + 4H_2O \quad (1)$$

The poorly crystallized niobate has a Na:Nb ratio of about 1.2 and is possibly composed of $Nb_6O_{19}{}^{8-}$ units, as evidenced by the XRD pattern in Figure 2, or the similar species of edge-sharing NbO_6 octahedra, as indicated by the Raman and UV−vis spectra in Figures 8 and 9. In the subsequent stages, the crystallized fibers with monoclinic lattice, $Na_2Nb_2O_6 \cdot {}^2/_3H_2O$, form and grow from the niobate of poor crystallinity, typically Nb-*80*, as shown in Figure 1, and the reaction can be expressed as:

$$Nb_6O_{19}{}^{8-} + 6Na^+ + 3H_2O \rightarrow 3Na_2Nb_2O_6 \cdot {}^2/_3H_2O + 2OH^- \quad (2)$$

The structure of the monoclinic $Na_2Nb_2O_6 \cdot {}^2/_3H_2O$ is metastable, and this observation is supported by thermodynamic analysis.[15,56] A stable structure of $NaNbO_3$ forms at the expense of the fibers in the final stage of the reaction:

$$3Na_2Nb_2O_6 \cdot {}^2/_3H_2O \rightarrow 6NaNbO_3 + 2H_2O \quad (3)$$

Actually, this reaction mechanism could also be used to interpret the synthesis reactions of SOMS solids. Generally, these syntheses start with niobium alkoxide, which hydrolyzes in the reaction systems.[13−15,56,58] The hydrolytes should consist of NbO_6 octahedra and have poor crystallinity or even be amorphous. In a concentrated NaOH solution and under hydrothermal conditions, the octahedral molecular sieves with NaO_6 and NaO_6 units in their framework could form and grow from the hydrolytes with a poor long distance order. However, the reaction product in this step is kinetic dependent and sensitive to the temperature. We can obtain high-purity fibers by optimizing the temperature and the reaction time. In the reaction systems reported previously,[13−15,56,58] the organic molecules from the alkoxide may stabilize the metastable SOMS solids so that they were obtained after relative long reaction periods.

4.3. The Structure and Structural Evolution. At a hydrothermal reaction temperature of 180 °C, we have been able to observe the amazing structural evolution in a practical period of the reaction. During the reaction course, niobates form and undergo sequential phase transitions, accompanied by morphological and compositional changes. Indeed, there are substantial difficulties in determining the niobate structures by a single technique, such as XRD, TEM, or ^{23}Na MAS NMR, alone. By employing a number of techniques including diffraction, imaging, vibrational and electronic spectroscopy, and NMR, we acquire comprehensive information about the structure of these niobates.

According to the results of XRD, SEM, and NMR, the samples Nb-*30*, Nb-*60*, Nb-*80*, Nb-*100*, Nb-*140*, and Nb-*160* are intermediates containing more than one phase. For instance, the SEM images show clearly that Nb-*100*, Nb-*140*, and Nb-*160* are the mixtures of niobate fibers and other particles (irregular particles or cubes). These intermediates from Nb-*30* to Nb-*80* possess irregular particle shape. There are two sodium niobates in the present study that possess regular morphologies. The Nb-*120* is identified by XRD, being pure microporous $Na_2Nb_2O_6 \cdot {}^2/_3H_2O$ fibers of monoclinic lattice (*C*2/c), and this structure is also supported by the results of HRTEM and ^{23}Na MAS NMR. The Nb-*180* is identified by XRD, being pure $NaNbO_3$ cubes of tetragonal lattice (*P*4/*mbm*). Nb-*140* and Nb-*160* are mixtures of fibers and cubes. A noticeable feature of the structural evolution is, in reactions 2 and 3, there is no similarity between the reactant and product in terms of particle shape and crystallinity. The image of Figure 1e illustrates that the fibers form outside the irregular niobate grains, which should be dissolved and provide the source of NbO_6 or clusters of NbO_6 for the growth of the fibers. ^{23}Na NMR results have indicated that sodium bonded to oxygen atoms in niobate species and water molecules exist in this sample. Part of the sodium ions in reaction 2 exists in distorted octahedral sites in framework rather than as free cations (see Scheme 1 and ref 14). Fiber growth could be viewed as assembling NbO_6 or clusters of NbO_6 and NaO_6 units. The well-crystallized fibers seem to be a thermodynamically more stable phase as compared to the poorly crystallized niobate, so that once crystal nuclei of this phase form, the fiber crystal grows rapidly while the niobate dissolves to provide source material for the fiber growth. The situation in reaction 3 is similar: the cubes appear outside the fibers and the latter dissolve to provide the source of NbO_6 or clusters of NbO_6 for the growth of the cubes, rather than a topochemical conversion, observed in phase transition from titanate fibers to anatase rods.[26,27] $NaNbO_3$ cubes are thermodynamically more stable than the crystal of the fibers.[56] It is worth pointing out that, although the fibers appear metastable and convert to cubes completely when the reaction with NaOH was prolonged for an hour (Figure 1), they are stable up to 400 °C. We summarized the structure evolution during the hydrothermal reaction in Scheme 1 in which the structures of the reactant, intermediates, and final product solids are expressed in assemblies of Nb−O polyhedra.

In Scheme 1, the structures are expressed in polyhedra (mainly octahedra) of niobium and oxygen, and Na cations are generally omitted, except for the fibers in which NaO_6 octahedra are shown in yellow. Concentrated NaOH ruptures the corner-sharing of niobium−oxygen polyhedra in the reactant Nb_2O_5, yielding intermediates with edge-sharing octahedral, which possess a poor crystallinity. The fibers form while the intermediate dissolves, providing the source of NbO_6 octahedra for fiber growth. Finally, the metastable fibers dissolve and NbO_6 octahedra assemble into $NaNbO_3$ cubes. It is noted that corner-sharing structures (Nb_2O_3 and $NaNbO_3$) exhibit optical properties different from those of the edge-sharing structures (the

(59) Jolivet, J. P. *Metal Oxide Chemistry and Synthesis: From Solution to Solid State*; Wiley: West Sussex, 2003; p 31.

intermediate and the fibers) as shown in Figure 9. This knowledge could be used to design niobate materials of desired optical properties.

V. Conclusion

The direct reaction between concentrated NaOH solution and metal oxide powder provides us with a precious opportunity to fabricate delicate structures of metal oxide and polyoxometalates. SEM can be employed to monitor the morphological evolution of the solid in such a reaction, and the SEM images provide a clear and direct picture of the reaction process. In the reaction between NaOH solution and Nb_2O_5, the corner-sharing of NbO_7 decahedra and NbO_6 octahedra is ruptured first. Next, in NaOH solution, the microporous fibers with monoclinic lattice, $Na_6H_2Nb_6O_{19}\cdot{}^2/_3H_2O$, crystallize and grow at the expense of the poorly crystallized niobate consisting of NbO_6 octahedra that are linked by edge-sharing. The delicate microporous molecular sieve structures of the fibers are confirmed by XRD, HRTEM, ^{23}Na MAS NMR techniques, and Li^+ ion exchange experiment and are consistent with those reported in the literature. Therefore, the fibers of $Na_6H_2Nb_6O_{19}\cdot{}^2/_3H_2O$ can be produced from a poorly crystallized or amorphous niobate obtained by other methods, such as hydrolysis of niobium alkoxide. By carefully optimizing the temperature and length of the reaction, one can achieve high-purity fibers with a delicate structure by direct reaction between concentrated NaOH solution and Nb_2O_5 powder. The optimal combination of the reaction temperature and time is at 180 °C for 120 min. Such a synthesis route is much simpler and easier to control than all of the syntheses of SOMS solids. Moreover, the simple composition of the reaction system and simple synthesis procedures make the analysis of the reaction mechanism feasible and the proposed mechanism reliable. The reaction mechanism could also be used to interpret the reactions in the synthesis reported in the literature. In addition to the simple procedures, another important feature of the synthesis of the present study is that selection of the fibril product is achieved by control of reaction kinetics. The final product for the continuing reaction at 180 °C is $NaNbO_3$ cubes. Such a structural conversion results in a remarkable change in light absorption. Therefore, this study is of importance for developing new function materials by wet-chemistry process.

Acknowledgment. Financial support from the Australian Research Council (DP0557945 and LX0454455), NSFC (90206043 and 50221201), and NCET (040219) of China is gratefully acknowledged. Y.H. acknowledges financial assistance from the NSERC, CFI, CRC, and PREA programs, and Prof. R. E. Wasylishen for kindly providing the WSOLIDS software package.

Supporting Information Available: Photoluminescence spectra of the samples. This material is available free of charge via the Internet at http://pubs.acs.org.

JA056301W